Sulfonated Triazine-Based Porous Organic Polymer for Excellent Proton Conductivity

Zhongping Li,[ab1*] Zhaohan Liu,[a1] He Li,[c1] Md Mahmudul Hasan,[a] Athchaya Suwansoontorn,[a] Gang Du,[a] Dongjin Wang,[a] Yuwei Zhang[d] and Yuki Nagao[a*]

[a]School of Materials Science, Japan Advanced Institute of Science and Technology, Ishikawa 923-1211, Japan.

[b]School of Energy and Chemical Engineering, Ulsan National Institute of Science and Technology, Ulsan 44919, Republic of Korea.

[c]State Key Laboratory of Catalysis, Dalian Institute of Chemical Physics, Chinese Academy of Sciences, Dalian, 110621, P. R. China.

[d] College of Chemistry, Jilin Normal University, Changchun, 130103, P. R. China.

[1]Z. Li, Z. Liu and H. Li contributed equally.

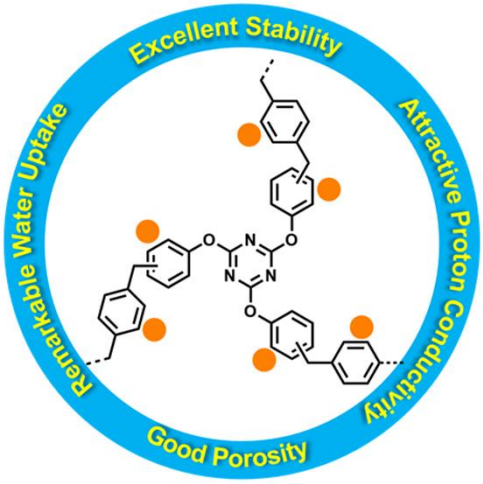

Keywords: Porous organic polymer， porosity, stability, water uptake, proton conductivity.

Abstract

Proton-exchange membrane fuel cells (PEMFCs) are a highly-promising green and environmental-friendly way to serve the sustainable development of human civilization. However, high-cost synthesis and polluted problems of the perfluorinated sulfonic-acid membranes are still not resolved. In this research, we designed and constructed porous organic polymers (POPs) with high porosity and excellent stability through the Friedel-Crafts acylation by using the commercial product as building blocks, and low-cost $FeCl_3$ as a catalyst through a simple operation. The POP-BP-1 was successfully synthesized by 1,4-bis(chloromethyl)benzene as a crosslinking agent and reactant. The POP-BP-TPOT was prepared via bringing in 2,4,6-triphenoxy-1,3,5-triazine (TPOT) as a building unit into the skeleton of POP-BP-1. Sulfonated POPs (S-POPs) were decorated with high-density sulfonic acid groups by postsulfonation. POP-BP-TPOT with abundant triazine units and sulfonic acid groups showed high water uptake. The sulfonated triazine-based polymer showed state-of-the-art high proton conductivity up to 10^{-2} S cm^{-1} at 25 °C and 95% relative humidity (RH), and low activation energy of 0.19 eV. Fuel cell test was also demonstrated using the polymer. This research suggests that the construction of S-POPs opens a suitable method to design high proton-conducting materials.

Introduction

In this century, energy consumption presents an urgent need owing to the rapid development of economization over the world. Proton-exchange membrane fuel cells (PEMFCs) are a green, sustainable, and environment-friendly energy resource and represents the next generation of energy saving. The development of PEMFC is of great significance.[1-5] The performance of the fuel cell depends largely on the characteristics of the proton exchange membrane. Electrolyte membranes should have good characteristics such as high proton mobility efficiency, and excellent chemical and physical stability under fuel cell operating conditions. In this process, various kinds of porous materials such as metal-organic frameworks (MOFs) and porous organic polymers (POPs), were well-designed as candidates for the proton-conductive electrolytes .[6-11]

Comparing traditional porous materials, POPs possessed many superior properties including high porosity, permanent pore, and easy decoration,[12-14] which was expanded to a large family incorporating conjugated microporous polymers (CMPs),[15] covalent organic frameworks (COFs),[16] porous aromatic frameworks (PAFs),[17] and hypercrosslinked polymers (HCPs).[18] Particularly, POPs were usually linked by strong covalent bonds to offer excellent chemical stability.[19-20] Based on these features, POPs have realized multi-functional platforms such as gas uptake,[21-26] catalysts,[27-31] chemical sensors,[32-36] and proton conduction carrier.[37-41]

The last five years has witnessed a rapid development of proton-conducting POPs owing to their pre-designable porous structure.[39-45] The POPs possess high porosity to load the high-density proton source, and permanent pore structure that can provide proton transportation channels. [8-9] To set up a proton-conducting system, loading proton sources such as imidazole, triazole, phosphoric acid, and sulfonic acid derivatives, into the pore is an effective and practical way. [9-11, 37-38] For example, the highly porous COF membrane loaded with large amounts of imidazole for excellent proton conduction (4.37×10^{-3} S cm^{-1}).[9] The post-functional process has been used to integrate sulfonic acid groups into networks via chlorosulfonic acid as a low-cost and high-efficiency reactant, which provides a new way to locate high-density sulfonic acid units on the networks to enhance water uptake and proton conductivity.[39-40, 42-45] The super-highly porous PAF-1 was used to qualify the large capacity sulfonic acid groups for proton conductivity up to 1.6×10^{-1} S cm^{-1} at 80 °C and 95% RH.[43] The improvement of proton-conductivity in relative humidity (RH) condition has highly relied on water uptake and the amount of proton source.[42-45] We are interested in sulfonated porous organic polymers owing to not only their excellent water adsorption capacity through the hydrogen bond interaction but also good ionization ability of protons from sulfonic acids as a strong organic acid. [46] With these in mind, POP-BP-1 with high porosity and excellent stability was successfully synthesized by 1,4-bis(chloromethyl)benzene as a crosslinking agent and reactant through the Friede-Crafts acylation by using

$FeCl_3$ as a catalyst via a simple operation. To increase water capture ability, triazine units (2,4,6-triphenoxy-1,3,5-triazine: TPOT) were inset into the skeleton of POP-BP-TPOT by the same synthesized way (Scheme 1). Interestingly, POP-BP-TPOT indicated high porosity and remarkable chemical stability, which offered a better circumstance for postsulfonation. The water uptake of sulfonated triazine-based polymer, S-POP-BP-TPOP, was improved by holding up high-density sulfonic acid groups and triazine units in the network. Interestingly, S-POP-BP-TPOP showed high conductivity up to 10^{-2} S cm^{-1} under 25 °C and 95% RH and lower activation energy of 0.19 eV.

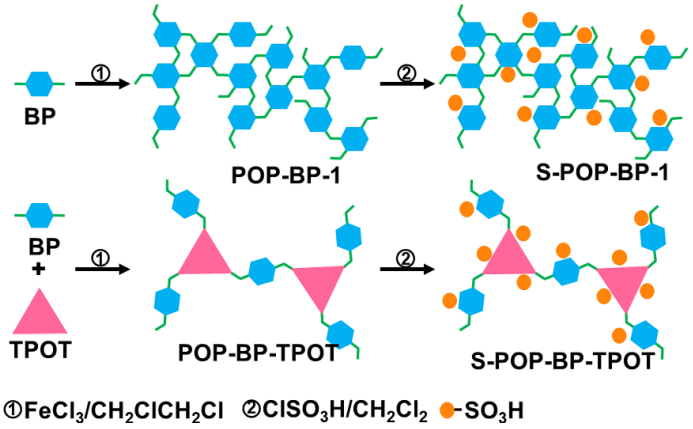

Scheme 1. Design and synthesis scheme of POPs and S-POPs.

Results and discussion

POPs can be prepared with high yield via Friedel–Crafts alkylation under $FeCl_3$ as a catalysis, which is a reliable method to synthesize highly porous networks.[47-49] The postsulfonation has been used to afford sulfonated POPs by chlorosulfonic acid as a post modified reagent.[42-45] The targeted polymers were fully characterized by Fourier transform infrared spectroscopy (FT-IR), thermogravimetric analysis (TGA), nitrogen and water adsorption, powder X-

ray diffraction measurements (PXRD), energy-dispersive X-ray spectroscopy (EDS) mapping, elemental analysis, Field Emission Scanning Electron Microscopes (FE SEM) and X-ray photoelectron spectroscopy (XPS). We investigated FT-IR measurement to observe the structure of polymers. There are obvious –CH_2– peaks around 2923 and 3003 cm^{-1} for POP-BP-1, around 2920 and 3025 cm^{-1} for POP-BP-TPOT (Figure 1), which are synthesized through Friedel–Crafts alkylation, respectively. POP-BP-TPOT displayed strong peaks around 1375 cm^{-1} that attribute to –C=N– signals of triazine units (TPOT). The strong new peaks at 1169 cm^{-1} for S-POP-BP-1, and 1166 cm^{-1} for S-POP-BP-TPOT (Figure 1), respectively, belonged to stretching modes of the S=O=S structure. These results indicate that the sulfonic acid group was successfully introduced into the network through the post-synthesis process.

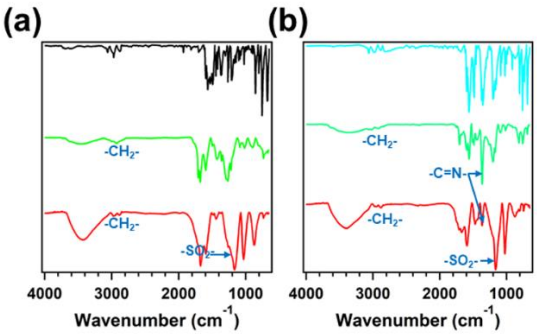

Figure 1. Fourier transform infrared spectra of (a) BP (black curve), POP-BP-1 (green curve) and S-POP-BP-1 (red curve), (b) TPOT (sky-blue curve), POP-BP-TPOT (green curve) and S-POP-BP-TPOT (red curve).

We also measured XPS for S-POPs. XPS results of S-POP-BP-TPOT indicated N 1s signal of triazine units at 398.1 eV (Figure 2). S-POPs displayed S $2p_{3/2}$ and S $2p_{1/2}$ signals around 168.4 and 169.6 eV. These data further suggested the presence of sulfonic acid groups in the frameworks. There is no

Fe signal in either POPs or S-POPs, which can eliminate the effects of the catalyst. EDS Elemental mapping of polymers was observed for POPs and S-POPs (Figure S1a-d). In Figure S1c-d, there is obvious information of N element, which belonged to triazine units of POP-BP-TPOT and S-POP-BP-TPOT. S-POPs showed a relatively uniform distribution of S and O elements (Figure S2b and 2d), which created a good environment for applications. The elemental analysis was measured for amounts of C, N, S, and H for POPs in Table S1. The S amount of S-POP-BP-1 and S-POP-BP-TPOT was observed at which indicated sulfonic acid of 23 and 30 wt%, respectively. Ion exchange capacity (IEC) of S-POPs was estimated at 2.8 and 3.6 mmol g^{-1} by acid–base titration, which was very closed to the elemental analysis results. S-POP-BP-TPOT showed rich sulfonic acid units in the skeleton, which attributed oxygen atoms serve as electron-donating groups to active aromatic ring for sulfonation.

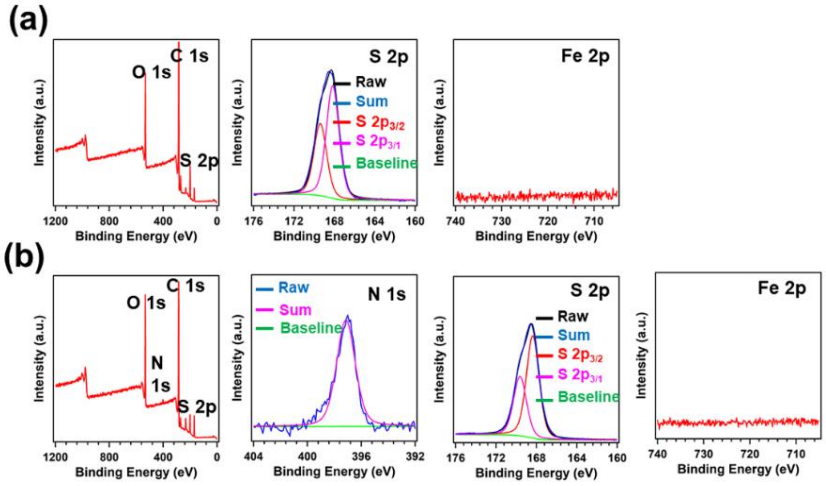

Figure 2. X-ray photoelectron spectroscopy (XPS) spectra of (a) S-POP-BP-1 and (b) S-POP-BP-TPOT.

Powder X-ray diffraction measurements (PXRD) of polymers suggested their amorphous networks (Figure S2). FE SEM images indicated their

aggregated particle morphology (Figure S3). We inspected the thermal stability of the polymers by thermogravimetric analysis (TGA) under nitrogen atmosphere (Figure S4). The backbone of POP-BP-1 indicated its excellent chemical stability and kept up to 350 °C without any decomposition (Figure S4a). The triazine-based POPs also remained 300 °C (Figure S4b), which provides a premise for functionalization.

The permanent porosities of POPs and S-POPs were recorded by nitrogen adsorption measurements at 77 K. All porous materials indicated type I isotherm with sharp uptake observed in the low pressure (Figure 3a-b), which is a representative character of micro-porosity according to the IUPAC classification. POP-BP-1 and POP-BP-TPOT showed Brunauer–Emmett–Teller (BET) surface area of 995 and 395 $m^2\ g^{-1}$, respectively. Comparing the original POPs, S-POP-BP-1 and S-POP-BP-TPOT exhibited a lower surface area of 657, and 93 $m^2\ g^{-1}$ in Figure 3a-b, respectively. The total pore volume was calculated from nitrogen gas adsorbed at P/P_0 = 0.99 of POPs. The total pore volume of sulfonated polymers was 1.35 $cm^3\ g^{-1}$ (POP-BP-1) and 0.62 $cm^3\ g^{-1}$ (POP-BP-TPOT), respectively, which is also higher than that of S-POP-BP-1 (0.95 $cm^3\ g^{-1}$) and S-POP-BP-TPOT (0.27 $cm^3\ g^{-1}$). S-POPs showed lower porosity, which suggested the sulfonic acid units possessed the network. All the prepared polymers are microporous materials according to their pore size distributions calculated by Non-local density functional theory (NLDFT) method (Figure 3c and d).

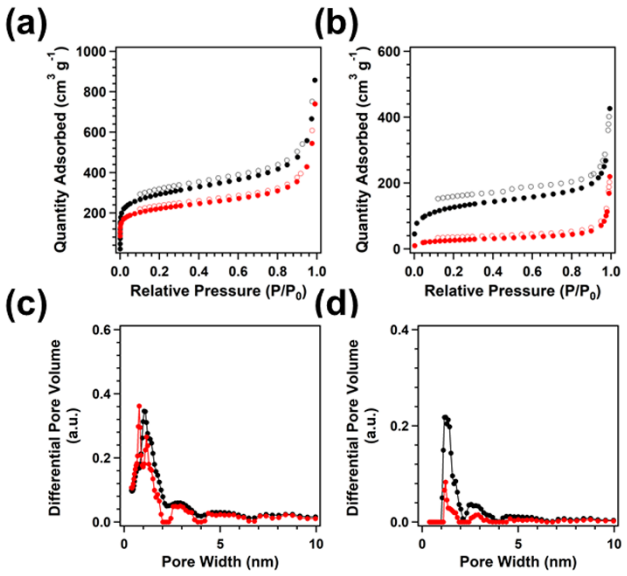

Figure 3. Nitrogen adsorption curves of (a) POP-BP-1 and S-POP-BP-1, (b) POP-BP-TPOT and S-POP-BP-TPOT. Pore size distribution of (c) POP-BP-1 and S-POP-BP-1, (d) POP-BP-TPOT and S-POP-BP-TPOT (POPs: black curves; S-POPs: red curves).

We investigated the chemical stability of POPs. All samples were dispersed in tetrahydrofuran (THF), water, and aqueous HCl (1 M) and NaOH (1 M) solutions, respectively, at 25 °C for 72 h. The POPs samples retained the microporous characters (Figure 4a-b) and the BET surface area slightly changed (Table S2). FT-IR spectra indicated all samples retained the vibration bands, which is the same as those of as-synthesized POPs (Figure 4c-d). Interestingly, these results indicated POP-BP-1 and POP-BP-TPOT exhibited excellent chemical stability, which is an important key for practical application.

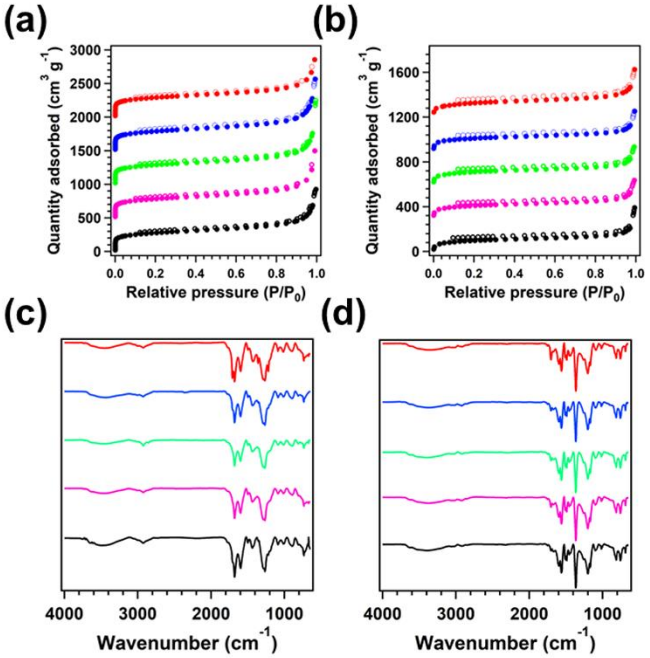

Figure 4. Nitrogen adsorption curves of (a) POP-BP-1 and (b) POP-BP-TPOT. FT IR spectra of (c) POP-BP-1 and (d) POP-BP-TPOT. (As-synthesized: red curve; THF: blue curve; water: green curve; 1 M HCl: purple curve; 1 M NaOH: black curve).

Humidity exerted a paramount significance on the proton-transport system owing to the improvement and strength of proton-exchange/transport efficiency. We investigated water vapor sorption for all polymers at 298 K (Figure 5). POP-BP-1 was constructed by hydrophobic aryl and alkyl groups, which induced their poor water adsorption capacity of 9.9 mmol g^{-1} at P/P_0 = 0.95 (Figure 5a). The water uptake ability of POP-BP-TPOT was enhanced up to 13.6 mmol g^{-1} through introducing triazine units into the skeleton in Figure 5a-b, which indicated triazine groups exhibited hydrophilic interaction towards to water molecules. After the sulfonated function, S-POP-BP-1 with sulfonic acid groups on the network further enhanced water uptake up to 22.8 mmol g^{-1}, which is two times that of original polymers. Interestingly, S-POP-BP-TPOT greatly enhanced water uptake up to 36.7 mmol g^{-1}, which gave the credit to the

stronger hydrogen bond interaction between the sulfonic acids and water molecules. These results are also higher than that of reported POPs.[42-45]

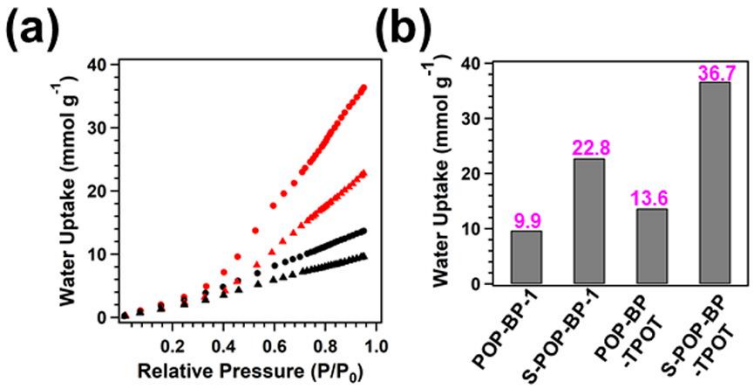

Figure 5. Water adsorption isotherms of (a) POP-BP-1 (▲), S-POP-BP-1 (▲), POP-BP-TPOT (●) and S-POP-BP-TPOT (●) at 298 K; (b) Comparison of water uptake of POPs and S-POPs.

The hydrophilic structure and high-density sulfonic acid units were successfully embedded in the network. The porous membranes also possessed permanent pore structure, which afforded the proton transfer channel. We inspected the proton conductivity of polymers under different humidity from 40 to 95% RH at 25 °C. As we can see in Figure 6a and S5a, S-POP-BP-1 strengthened proton-conducting values with the increase of humidity. At 40% RH and 25 °C, S-POP-BP-1 showed proton conductivity of 1.2×10^{-6} S cm^{-1}. When the humidity increased to 60, 70, and 80%, the proton conductivity values were strengthened for 2.7×10^{-5}, 7.3×10^{-5} and 2.8×10^{-4} S cm^{-1} at 60%, 70% and 80% RH under 25 °C (Figure S5a), respectively. The highest conductivity of S-POP-BP-1 was observed at 4.6×10^{-3} S cm^{-1} at 95% RH, which is 2.4 orders of magnitudes greater than that of POP-BP-1 (Figure 6c). Anchored in triazine units in the skeleton, POP-BP-TPOT displayed the value at 8.4×10^{-5}

S cm^{-1} at 95% RH under 25 °C (Figure S6c), which is more than 42 times than that of POP-BP-1 (Figure S6a). This enhancement is attributed to the hydrophilic structure of triazine units. The excellent conductivity of S-POP-BP-TPOT was as high as 1.5 × 10^{-2} S cm^{-1} at 95% RH under 25 °C (Figure S5b), which is three times that of S-POP-PB-1 and 8.0 orders magnitudes greater than that of POP-BP-1. These results indicated sulfonic acid structure greatly enhanced proton transmission capacity. That value is comparable to those of reported proton-conductive materials such as 1S (1.30×10^{-2} S cm^{-1}, 90% RH and 30 °C),[39] SBO-CMP-1 (4.15 × 10^{-3} S cm^{-1}, 100% RH and 30 °C),[40] SBO-CMP-2 (1.16 × 10^{-3} S cm^{-1}, 100% RH and 30 °C),[40] NUS-9 (R) (1.24 × 10^{-2} S cm^{-1}, 97% RH and 25 °C),[41] SPAF-1(0.5) (9.8 × 10^{-4} S cm^{-1}, 100% RH and 25 °C) and SPAF-1(1.25) (1.8 × 10^{-4} S cm^{-1} at 100% RH and 25 °C),[43] and PCF-1-SO_3H (2.6 × 10^{-2} S cm^{-1}, 95% RH and 25 °C).[44] Comparing current standard materials such NR-211 (7.0 × 10^{-2} S cm^{-1}, at 25 °C and 100% RH) [50] and NR-117 (7.5 × 10^{-2} S cm^{-1}, at 25 °C and 98% RH), [51] this result also shows high conductivity performance.

The time-dependent proton conductivity for S-POP-BP-1 and S-POP-BP-TPOT has been checked and there is negligible change in proton conductivity value even after 6 h (Figure S7a-b). The structure of S-POP-BP-1 and S-POP-BP-TPOT was also no change, which was confirmed by FT-IR spectra (Figure S7c-d). We used the Fenton's reagent (30% H_2O_2, 30 ppm $FeSO_4$) to treat POPs and S-POPs for 72 h. The retention of the respective sulfonic acid groups

was confirmed by FT-IR spectroscopy (Figure S8). These results indicated S-POPs displayed excellent proton conductivity and remarkable stability of the polymer membranes in the working condition.

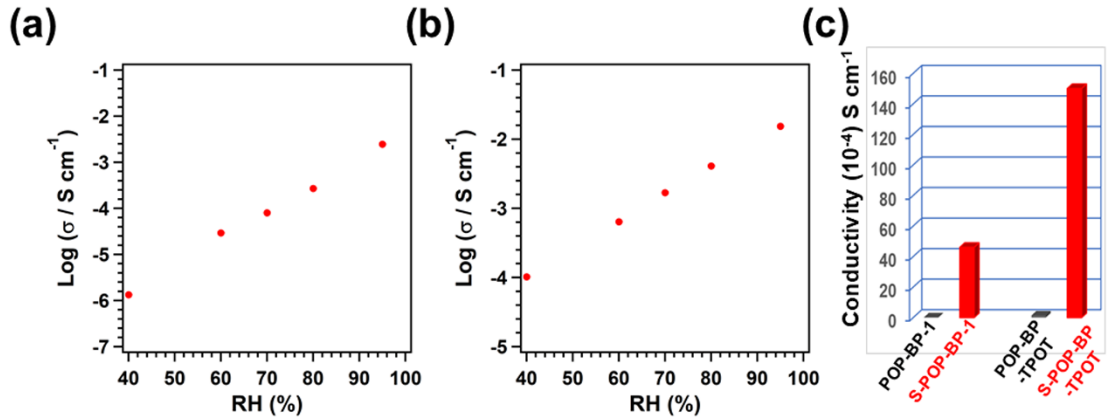

Figure 6. Proton conductivities of (a) S-POP-BP-1 and (b) S-POP-BP-TPOT measured under different RHs and 25 °C. (c) Comparison of proton conductivities of POPs and S-POPs under 95% RHs and 25 °C.

Encouraged by the high proton conductivity of S-POP-BP-TPOT, we have measured polarization curves of S-POP-BP-TPOT under the H_2/O_2 fuel cell working conditions in Figure S9. The fuel cell performance was carried out under 100% RH condition at 40 °C and 60 °C, respectively. In both temperature condition the open circuit voltage (OCV) showed around 0.55 V, which was smaller than those of 1ES (0.72 V; 80 °C and 100% RH),[42] PA@TpBpy-ST (0.68 V; 50 °C and dry gas) and PA@TpBpy-MC (0.92 V; 50 °C and dry gas), [52], and a Nafion MEA (1.01 V; 80 °C and 100% RH).[53] The potential-voltage polarization curve of S-POP-BP-TPOT displayed a maximum power density of 50 mW cm^{-2} at 60 °C.

We investigated the activation energy (Ea) of POPs and S-POPs to explore the proton conduction mechanistic insight from Arrhenius plots measurement

at various temperatures (Figure 7). The Ea of POP-BP-1 was 0.69 eV. The S-POP-BP-1 showed a lower value of 0.28 eV, which indicated that the proton conduction possesses via the Grotthuss mechanism owing to the lower activation energy of sulfonated polymers. For triazine polymer, S-POP-BP-TPOT displayed a lower value of 0.19 eV, which originated from excellent water uptake of triazine and sulfonic acid units in the network. This value is better than those of the reported POPs and commercially proton-conductive materials such as Nafion (0.22 eV),[54] SBO-CMP-1 (0.32 eV) and SBO-CMP-2 (0.40 eV),[40] 1S (0.32 eV),[39] and NUS-9 (R) (0.20 eV).[41]

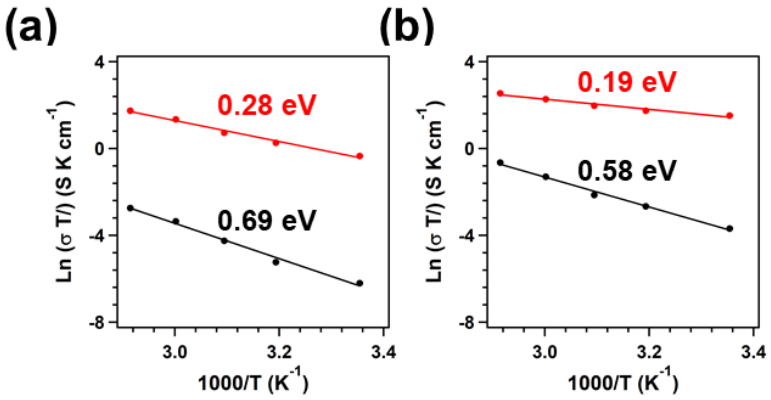

Figure 7. Arrhenius plots for (a) POP-BP-1 and S-POP-BP-1, (b) POP-BP-TPOT and S-POP-BP-TPOT (POPs: black and S-POP: red).

Conclusions

In this research, we designed and synthesized triazine skeleton porous organic polymers POP-BP-TPOT with high porosity, excellent stability, and good water uptake ability by using commercial reagents and low-cost $FeCl_3$ as a catalyst through a simple operation. Sulfonated triazine POPs were formed via pore surface engineering through chlorosulfonic acid as a post-modified

reagent. With the improvement of water uptake through modified triazine and sulfonic acid groups on the skeleton, S-POP-BP-TPOT indicated proton conductivity up to 10^{-2} S cm^{-1} under at 25 °C and 95% RH. The activation energy of S-POP-BP-TPOT showed the lowest activation energy of 0.19 eV, which is lower than those of commercial products and most reported POPs. These results offer a new way to extend structural designs for high proton-conducting materials. Currently, the new design and synthesis of functional POPs for energy and environment fields are underway in our laboratory.

Experimental section

Materials and methods

2,4,6-Triphenoxy-1,3,5-triazine, 1,4-bis(chloromethyl)benzene, chlorosulfonic acid, anhydrous $FeCl_3$, acetone, methanol, and other materials were obtained from TCI, Wako, and Sigma-Aldrich. Fourier transforms Infrared (FT IR) spectra were measured from 650 to 4000 cm^{-1} by using the FT IR spectrometer (Nicolet 6700; Thermo Fisher Scientific Inc.). Elemental analyses were carried out on a CHN element analysis EMGA-930, HORIBA, Japan. The elemental sulfur content was carried out on an Elementar model vario EL cube analyzer. Field emission scanning electron microscope was performed on HITACHI Miniscope TM3030. Energy-dispersive X-ray spectroscopy (EDS) mapping was measured by TM3030Plus miniscope. The X-ray photoelectron spectroscopy (XPS) measurement was implemented on a DLD spectrometer (Kratos Axis-Ultra; Kratos Analytical Ltd). The Brunauer-Emmett-Teller (BET) method was utilized

to calculate the specific surface areas through nitrogen sorption curves that measured at 77 K by BELSORP-max. The pore size was calculated from the sorption curve via the non-local density functional theory (NLDFT) method. Water sorption was recorded by Micromeritics ASAP 2020. Powder x-ray diffractometer (XRD) patterns were recorded on a fully automatic horizontal multi-purpose x-ray diffractometer (Rigaku Smartlab; Rigku Corp.).

Synthetic procedures

Synthesis of POP-BP-1: The POP-BP-1 was prepared by the reported method.[39-40] 1,4-Bis(chloromethyl)benzene (BP) (70 mg, 0.49 mmol), anhydrous $FeCl_3$ (161 mg, 0.97 mmol) and 1,2-dichloroethane 4 mL were added into the flask. To disperse this system, it was stirred for 2 minutes and then degassed through three freeze-pump-thaw cycles. Under the Ar atmosphere, the system stayed at 80 ºC for 48 h. Then, the system was cooled down to room temperature and the powder was collected and washed by water and acetone, soxhlet by methanol for 12 h, and dried in vacuum. The polymer was dispersed in 1M HCl 50 mL and stirred overnight, filtered and washed by water and acetone, and dried under vacuum at room temperature for 24 hours to afford brown powder in 95% isolated yield.

Synthesis of POP-BP-TPOT: 1,4-Bis(chloromethyl)benzene (BP) (44 mg, 0.25 mmol), 2,4,6-triphenoxy-1,3,5-triazine (60 mg, 0.17 mmol), anhydrous $FeCl_3$ (84 mg, 0.50 mmol) and 1,2-dichloroethane 4 mL were added into the flask. To disperse this system, it was stirred for 2 minutes and then degassed through

three freeze-pump-thaw cycles. Under the Ar atmosphere, the system stayed at 80 ºC for 2 d. Then, the system was cooled down to room temperature and the powder was collected and washed by water and acetone, soxhleted by methanol overnight, and dried in vacuum. Then, the polymer was dispersed in 1M HCl of 50 mL, filtered and washed by water and acetone. We used 1M NaOH of 25 mL to treat polymer for 1 h. Finally, the polymer was filtered and washed by water and acetone, then dried under vacuum at room temperature for 24 h to afford brown powder in 75% isolated yield (brown powder).

Synthesis of S-POPs: The S-POP-BP-1 was prepared by the reported method. [44-45] The POP-B (200 mg) in dichloromethane 10 mL was stirred at an ice-water bath for server mins. Then chlorosulfonic acid 2.5 mL was slowly added into this system. The system gradually recovered to room temperature and stirred for 7 d. Finally, the mixture was slowly poured into ice water. Until it came to room temperature, S-POP-BP was collected and washed by water, methanol, and acetone, dried under vacuum for 24 h (247 mg). We used the same procedure to prepare S-POP-BP-TPOT.

Chemical stability measurement

The polymers (POP-BP-1 and POP-BP-TPOT) 50 mg were dispersed in water, THF, 1 M NaOH and 1 M HCl at room temperature for 72 h. Finally, the polymers were collected and washed by a large amount of water and acetone, and dried in vacuum for 24 h. (For POP-BP-TPOT polymer in HCl, we used little NaOH to treat it, and then washed by water and acetone).

Proton conductivity measurements

S-POPs were ground and pressed to prepare pellets under high pressure. Then the pellets were equipped with two home-made Pt electrodes with two platinum wires connecting the impedance spectroscopy system. Proton conductivity of S-POPs pellets was recorded through impedance spectroscopy pellets by using a frequency response analyzer (SI1260; Solartron Analytical) equipped with a high-frequency dielectric interface. Different RH and temperature were manipulated via a computer-controlled environmental test chamber (SH-221; Espec Corp.). We recorded impedance results by frequencies between 1 Hz and 10 MHz, with an applied alternating potential of 50 mV. Proton conductivity (σ) was calculated as, $\sigma = L / (R \times S)$, where R denotes the resistance value obtained from the impedance, S and L respectively stand for the contact electrode area and the thickness of the pellet. The activation energy (Ea) of S-POPs was calculated as, $\sigma_T = \sigma_0 \times \exp(-Ea / (k_B \times T))$, where σ is proton conductivity, σ_0 is pre-exponential factor, k_B is the Boltzmann constant, and T is temperature.

Polarization curve measurements for full cell test

Polarization curves were evaluated using a home-made fuel cell test system with a single cell (ElectroChem, Inc.) at 40 °C. The sample was used in the form of pellets as it is insoluble in solvent and could not be formed into a film.[55] A commercially available catalyst layer with 20 wt.% Pt/C (EC-E20-10-7; TOYO Co.) was used for both the anode and the cathode. 5% Nafion dispersion solution

(DE521 CS; FUJIFILM Wako Pure Chemical Co.) was sprayed as an ionomer.[56] All assemblies were inserted between two graphite plates with serpentine flow fields. The fully humidified hydrogen and oxygen gases of 100 sccm were fed, respectively, into the cell at the anode and cathode. The mass flow controller was used to control the constant flow-rates for the fuel cell. The current–potential (I–V) curve was measured by an Electronic Load unit (PLZ164WA; Kikusui Electronics Co.)

Conflicts of interest

There are no conflicts to declare.

Acknowledgements

Z.L. and Y.N. appreciate the support by JSPS KAKENHI grant number JP18J13699 and JP18K05257. Y.Z. acknowledges the support by Natural Science Foundation of China (21805110).

References

1. Hickner, M. A.; Ghassemi, H.; Kim, Y. S.; Einsla, B. R.; McGrath, J. E. Alternative Polymer Systems for Proton Exchange Membranes (PEMs). *Chem. Rev*. **2004**, *104*, 4587−4612.
2. Nagao, Y. Proton-Conductivity Enhancement in Polymer Thin Films. *Langmuir* **2017**, *33*, 12547−12558.

3. Peckham, T. J.; Holdcroft, S. Structure-Morphology-Property Relationships of Non-Perfluorinated Proton-Conducting Membranes. *Adv. Mater*. **2010**, *12*, 4667−4690.
4. Nagao, Y. Progress on highly proton-conductive polymer thin films with organized structure and molecularly oriented structure. *Sci. Tech. Adv. Mater.* **2020**, *21*, 79−91.
5. Yao, H.; Zhang, Y.; Liu, Y. You, K.; Song, N.; Liu, B.; Guan, S. Pendant-group cross-linked highly sulfonated co-polyimides for proton exchange membranes. *J. Membr. Sci.* **2015**, 480, 83–92.
6. Horike, S.; Umeyama, D.; Kitagaw, S. Ion Conductivity and Transport by Porous Coordination Polymers and Metal-Organic Frameworks. *Acc. Chem. Res*. **2013**, *11*, 2376−2384.
7. Yoon, M.; Suh, K.; Natarajan, S.; Kim, K. Proton Conduction in Metal-Organic Frameworks and Related Modularly Built Porous Solids. *Angew. Chem. Int. Ed*. **2013**, *52*, 2688−2700.
8. Phang, W. J.; Jo, H.; Lee, W. R.; Song, J. H.; Kim, B. S.; Hong, C. S. Superprotonic Conductivity of a UiO-66 Framework Functionalized with Sulfonic Acid Groups by Facile Postsynthetic Oxidation. *Angew. Chem. Int. Ed*. **2015**, *54*, 5142–5146.
9. Xu, H.; Tao, S.; Jiang, D. Proton Conduction in Crystalline and Porous Covalent Organic Frameworks. *Nat. Mater*., **2016**, *15*, 722–726.
10. Ma, H.; Liu, B; Li, B.; Zhang, L.; Li, Y.; Tan, H. Q.; Zang, H. Y.; Zhu, G.

Cationic Covalent Organic Frameworks: A Simple Platform of Anionic Exchange for Porosity Tuning and Proton Conduction. *J. Am. Chem. Soc*. **2016**, *18*, 5897–5903.

11. Ranjeesh, K. C.; Illathvalappil, R.; Veer, D. S.; Peter, J.; Wakchaure, V. C.; Goudappagouda; Raj, K. V.; Kurungot, S.; Babu, S. S. Imidazole-Linked Crystalline Two-Dimensional Polymer with Ultrahigh Proton-Conductivity. *J. Am. Chem. Soc*. **2019**, *141*, 14950−14954.
12. Xu, Y.; Jin, S.; Xu, H.; Nagai, A.; Jiang, D. Conjugated Microporous Polymers: Design, Synthesis and Application. *Chem. Soc. Rev*. **2013**, *42*, 8012–8031.
13. Zhang, Y.; Riduana, S. N. Functional Porous Organic Polymers for Heterogeneous Catalysis. *Chem. Soc. Rev*. **2012**, *41*, 2083–2094.
14. Kaur, P.; Hupp, J. T.; Nguyen, S. T. Porous Organic Polymers in Catalysis: Opportunities and Challenges. *ACS Catal*. **2011**, *7*, 819–835.
15. Cooper, A. I. Conjugated Microporous Polymers. *Adv. Mater*. **2009**, *21*, 1291–1295.
16. Huang, N.; Wang, P.; Jiang, D. Covalent organic frameworks: a materials platform for structural and functional designs. *Nat. Rev. Mater*. **2016**, *1*, 16068.
17. Yuan, Y.; Zhu, G. Porous Aromatic Frameworks as a Platform for Multifunctional Applications. *ACS Cent. Sci.* **2019**, *3*, 409–418.
18. Tan, L.; Tan, B. Hypercrosslinked Porous Polymer Materials: Design,

Synthesis, and Applications. *Chem. Soc. Rev*. **2017**, *46*, 3322–3356.

19. Huang, N.; Zhai, P.; Xu, H.; Jiang, D. Stable Covalent Organic Frameworks for Exceptional Mercury Removal from Aqueous Solutions. *J. Am. Chem. Soc*. **2017**, *139*, 2428.
20. Zhi, Y.; Li, K.; Xia, H.; Xue, M.; Mu, Y.; Liu, X. Robust Porous Organic Polymers as Efficient Heterogeneous Organo-Photocatalysts for Aerobic Oxidation Reactions. *J. Mater. Chem. A* **2017**, *5*, 8697–8704.
21. Guan, X.; Li, H.; Ma, Y.; Xue, M.; Fang, Q.; Yan, Y.; Valtchev, V.; Qiu, S. Chemically Stable Polyarylether-Based Covalent Organic Frameworks. *Nat. Chem*. **2019**, *11*, 587–594.
22. Chen, Q.; Luo, M.; Hammershøj, P.; Zhou, D.; Han, Y.; Laursen, B. W.; Yan, C.-G.; Han, B.-H. Microporous Polycarbazole with High Specific Surface Area for Gas Storage and Separation. *J. Am. Chem. Soc*. **2012**, *134*, 6084–6087.
23. Li, Z.; Feng, X.; Zou, Y.; Zhang, Y.; Xia, H.; Liu, X.; Mu, Y. A 2D Azine-Linked Covalent Organic Framework for Gas Storage Applications. *Chem. Commun*. **2014**, *50*, 13825–13828.
24. Song, N.: Wang, T.: Yao, H.; Ma, T.; Shi, K.; Tian, Y.; Zou, Y.; Zhu, S.; Zhang, Y.; Guan, S. Construction and Carbon Dioxide Capture of Microporous Polymer Networks with High Surface Area Based on Cross-Linkable Linear Polyimides. *Polym. Chem.*, **2019**, *10*, 4611–4620.
25. Zhu, X.; Tian, C.; Veith, G. M.; Abney, C. A.; Dehaudt, J.; Dai, S. In Situ

Doping Strategy for the Preparation of Conjugated Triazine Frameworks Displaying Efficient CO_2 Capture Performance. *J. Am. Chem. Soc.* **2016**, *138*, 11497–11500.

26. Huang, N.; Wang, P.; Addicoat, M. A.; Heine, T.; Jiang, D. Ionic Covalent Organic Frameworks: Design of a Charged Interface Aligned on 1D Channel Walls and Its Unusual Electrostatic Functions. *Angew. Chem. Int. Ed.* **2017**, *56*, 4982.
27. Bhanja, P.; Modak, A.; Bhaumik, A. Porous Organic Polymers for CO_2 Storage and Conversion Reactions. *ChemCatChem* **2019**, *11*, 244–257.
28. Liu, M.; Zhou, B.; Zhou, L.; Xie, Z.; Li, S.; Chen, L. Nitroxyl Radical Based Conjugated Microporous Polymers as Heterogeneous Catalysts for Selective Aerobic Alcohol Oxidation. *J. Mater. Chem. A* **2018**, *6*, 9860–9865.
29. Zhi, Y.; Yao, Z.; Jiang, W.; Xia, H.; Shi, Z.; Mu, Y.; Liu, X. Conjugated Microporous Polymers as Heterogeneous Photocatalysts for Efficient Degradation of a Mustard-Gas Simulant. *ACS Appl. Mater. Interfaces* **2019**, *11*, 37578−37585.
30. Song, J.; Li, Y.; Cao, P.; Jing, X.; Faheem, M.; Matsuo, Y.; Zhu, Y.; Tian, Y.; Wang, X.; Zhu, G. Synergic Catalysts of Polyoxometalate@Cationic Porous Aromatic Frameworks: Reciprocal Modulation of Both Capture and Conversion Materials. *Adv. Mater*. **2019**, *31*, 1902444.
31. Sun, Q.; Dai, Z.; Liu, X.; Sheng, M.; Deng, F.; Meng, X.; Xiao, F.-S. Highly Efficient Heterogeneous Hydroformylation over Rh-Metalated Porous

Organic Polymers: Synergistic Effect of High Ligand Concentration and Flexible Framework. *J. Am. Chem. Soc*. **2015**, *137*, 5204−5209.

32. Li, Z.; Li, H.; Xia, H.; Ding, X.; Luo, X.; Liu, X.; Mu, Y. Triarylboron-Linked Conjugated Microporous Polymers: Sensing and Removal of Fluoride Ions. *Chem. Eur. J.* **2015**, *21*, 17355–17362.
33. Li, Z.; Huang, N.; Lee, K. H.; Feng, Y. Tao, S.; Jiang, Q; Nagao, Y.; Irle, S.; Jiang, D. Light-Emitting Covalent Organic Frameworks: Fluorescence Improving via Pinpoint Surgery and Selective Switch-On Sensing of Anions. *J. Am. Chem. Soc*. **2018**, *39*, 12374–12377.
34. Li, Z.; Zhang, Y.; Xia, H.; Mu, Y.; Liu, M. A Robust and Luminescent Covalent Organic Framework as a Highly Sensitive and Selective Sensor for the Detection of Cu^{2+} Ions. *Chem. Commun*. **2016**, *52*, 6613–6616.
35. Guo, L.; Wang, M.; Zeng, X.; Cao, D. Luminescent Porous Organic Polymer Nanotubes for Highly Selective Sensing of H_2S. *Mater. Chem. Front*. **2017**, *1*, 2643–2650.
36. Dong, J.; Tummanapelli, A. K.; Li, X.; Ying, S.; Hirao, H.; Zhao, D. Fluorescent Porous Organic Frameworks Containing Molecular Rotors for Size-Selective Recognition. *Chem. Mater*. **2016**, *28*, 7889–7897.
37. Chandra, S.; Kundu, T.; Kandambeth, S.; BabaRao, R.; Marathe, Y.; Kunjir, S. M.; Banerjee, R. Phosphoric Acid Loaded Azo (−N═N−) Based Covalent Organic Framework for Proton Conduction. *J. Am. Chem. Soc*. **2014**, *136*, 6570–6573.

38. Halder, A.; Ghosh, M.; Khayum M, A.; Bera, S.; Addicoat, M.; Sasmal, H. S.; Karak, S.; Kurungot, S.; Banerjee, R. Interlayer Hydrogen-Bonded Covalent Organic Frameworks as High-Performance Supercapacitors. *J. Am. Chem. Soc*. **2018**, *140*, 10941–10945.

39. Kang, D. W.; Lim, K. S.; Lee, K. J.; Lee, J. H.; Lee, W. R.; Song, J. H.; Yeom, K. H.; Kim, J. Y.; Hong, C. S. Cost-Effective, High-Performance Porous-Organic-Polymer Conductors Functionalized with Sulfonic Acid Groups by Direct Postsynthetic Substitution. *Angew. Chem. Int. Ed*. **2016**, *55*, 16123–16360.

40. Yang, S.; Ding, X.; Han, B. H. Conjugated Microporous Polymers with Dense Sulfonic Acid Groups as Efficient Proton Conductors. *Langmuir* **2018**, *26*, 7640–7646.

41. Peng, Y.; Xu, G.; Hu, Z.; Cheng, Y.; Chi, C.; Yuan, D.; Cheng, H; Zhao, D. Mechanoassisted Synthesis of Sulfonated Covalent Organic Frameworks with High Intrinsic Proton Conductivity. *ACS Appl. Mater. Interfaces* **2016**, *28*, 18505–18512.

42. Kang, D. W.; Song, J. H.; Lee, K. J.; Lee, H. G.; Kim, J. E.; Lee, H. Y.; Kim, J. Y.; Hong, C. S. A Conductive Porous Organic Polymer with Superprotonic Conductivity of a Nafion-Type Electrolyte. *J. Mater. Chem. A* **2017**, *5*, 17492–17498.

43. Klumpen, C.; Gödrich, S.; Papastavrou, G.; Senker, J. Water Mediated Proton Conduction in a Sulfonated Microporous Organic Polymer. *Chem.*

Commun. **2017**, *53*, 7592–7595.

44. Samanta, P.; Desai, A. V.; Anothumakkool, B.; Shirolkar, M. M.; Karmakar, A.; Kurungot, S.; Ghosh, S. K. Enhanced Proton Conduction by Post-Synthetic Covalent Modification in a Porous Covalent Framework. *J. Mater. Chem. A* **2017**, *5*, 13659–13664.
45. Li, Z.; Yao, Y.; Wang, D.: Suwansoontorn, A.; Hasan, M. MD.; Li, H.; Du, G.; Liu, Z.; Nagao, Y. *Mater. Chem. Front.,* doi.org/10.1039/D0QM00276C.
46. Paddison, S. J. The modeling of molecular structure and ion transport in sulfonic acid based ionomer membranes. *J. New. Mat. Electrochem. Systems*., **2001**, 4, 197-207.
47. Chaikittisilp, W.; Kubo, M.; Moteki, T.; Sugawara-Narutaki, A.; Shimojima, A.; Okubo, T. Porous Siloxane–Organic Hybrid with Ultrahigh Surface Area through Simultaneous Polymerization–Destruction of Functionalized Cubic Siloxane Cages. *J. Am. Chem. Soc*. **2011**, *133*, 13832–13835.
48. Wood, C. D.; Tan, B.; Trewin, A.; Niu, H.; Bradshaw, D.; Rosseinsky, M. J.; Khimyak, Y. Z.; Campbell, N. L.; Kirk, R.; Stockel, E.; Cooper. A. I. Hydrogen Storage in Microporous Hypercrosslinked Organic Polymer Networks. *Chem. Mater*. **2007**, *19*, 2034–2048.
49. Schwab, M. G.; Lennert, A.; Pahnke, J.; Jonschker, G.; Koch, M.; Senkovska, I.; Rehahnd, M.; Kaskel, S. Nanoporous Copolymer Networks through Multiple Friedel–Crafts-Alkylation–Studies on Hydrogen and Methane Storage. *J. Mater. Chem*. **2011**, *21*, 2131–2135.

50. Peron,J.; Mani, A.; Zhao, X.; Edwards, D.; Adachi, M.; Soboleva, T.; Shi, Z.; Xie, Z.; Navessin, T.; Holdcroft, S. Properties of Nafion NR-211 membranes for PEMFCs, *J. Membr. Sci.* **2010**, *356*, 44–51.

51. T. A. Zawodzinski, Jr, C. Derouin, S. Radzinski, R. J. Sherman, V. T. Smith, T. E. Springer and S. Gottesfeld, Water uptake by and transport through Nation 117 membranes, J. Electrochem. Soc., 1993, 140, 1041

52. Shinde, D. B.; Aiyappa, H. B.; Bhadra, M.; Biswal, B. P.; Wadge, P.; Kandambeth, S.; Garai, B., Kundu, T.; Kurungot, S.; Banerjee, R. A mechanochemically synthesized covalent organic framework as a proton-conducting solid electrolyte. *J. Mater. Chem. A*, **2016**, 4, 2682–2690.

53. Zhang, J.; Yang, Y.; Song, C.; Zhang, J.; Wang, H. PEM fuel cell open circuit voltage (OCV) in the temperature range of 23 °C to 120 °C. *J. Power Sources*, **2006**, *163*, 532–537.

54. Giulio, A.; Mario, C. Solid State Protonic Conductors, Present Main Applications and Future Prospects. *Solid State Ionics*, **2001**, *145*, 3–16.

55. Nagao, Y.; Matsui, J.; Abe, T.; Hiramatsu, H.; Yamamoto, H.; Miyashita, T.; Sata, N.; Yugami, H. Enhancement of Proton Transport in an Oriented Polypeptide Thin Film. *Langmuir* **2013**, *29*, 6798–6804.

56. Wang, Z.; Nagao, Y. Effects of Nafion impregnation using inkjet printing for membrane electrode assemblies in polymer electrolyte membrane fuel cells. *Electrochimica Acta*, **2014,** *129*, 343–347.